Separation of Single-Walled Carbon Nanotubes with Aromatic Group Functionalized Polymethacrylates and Building Blocks Contribution to the Enrichment

Xiaoyong Pan, Mary B. Chan-Park

School of Chemical and Biomedical Engineering, Nanyang Technological University, 62 Nanyang Drive, Singapore 637459, Singapore

Correspondence to: M. B. Chan-Park (E-mail: mbechan@ntu.edu.sg)

Received 5 October 2010; revised 11 April 2011; accepted 12 April 2011; published online 12 May 2011
DOI: 10.1002/polb.22265

ABSTRACT: We previously showed that in *N,N*-dimethylformamide (DMF), poly(9-anthracenylmethyl methacrylate) (PAMMA) and poly(2-naphthylmethacrylate) selectively disperse semiconducting and metallic single-walled carbon nanotubes (SWNTs), respectively. We have also proposed a new noncovalent polymer interaction based on photon induced dipole–dipole interaction to account for the metallicity-based selectivity. In this article, we investigate two other polymethacrylates, that is, poly(benzyl methacrylate) (PBMA) and poly(methylmethacrylate)-*co*-(9-anthracenylmethyl acrylate) (PMMA-*c*-PAMA) in the light of our previously proposed photon-induced dipole–dipole interaction. We find that PBMA and PMM-*c*-PAMMA in DMF show no metallicity selectivity. The different selective behavior of the four polymers in DMF manifests the decisive influence of the side aromatic group in determining their metallicity selectivity. The nonpreferential energy transfer from PMMA-*c*-PAMA to SWNTs and the nonoverlap of PBMA fluorescence (in the ultraviolet range) with nanotube absorption account for their nonselectivity of specific nanotube species. Further, the parallel relationship between the diameters of extracted tube species and the affinity between polymers and solvents suggests the leading role of the polymeric conformation on the diameter selectivity. A sufficient (i.e., 2 weeks) standing time of the SWNTs solution after sonication, during which the polymers presumably optimize their conformation to the SWNTs, was found to be essential to the enrichment. © 2011 Wiley Periodicals, Inc. J Polym Sci Part B: Polym Phys 49: 949–960, 2011

KEYWORDS: carbon nanotubes; fluorescence; separation techniques

INTRODUCTION Because of their superior electrical, mechanical, optical, chemical, and thermal properties,[1–9] single-walled carbon nanotubes (SWNTs) have, since their discovery in 1991,[10] attracted much research attention and substantial progress has been made. However, the realization of their potential application in microelectronic devices[11–15] has been severely hampered by the great challenge of obtaining pure metallic or semiconducting (met-/sem-) SWNTs.[16,17] The control of their electronic properties has been partially achieved in some synthetic methods but improvement is still highly desired for practical applications.[18] On the other hand, much research effort has been devoted to postsynthetic separation. Successful postsynthetic enrichment has been achieved by techniques such as ac dielectrophoresis,[19–21] anion exchange chromatography of DNA-assisted SWNT suspension,[22,23] and density gradient ultracentrifugation method,[24] and so forth. The scaling difficulty of these methods hinders their commercial application.

Metallicity-based chemical approaches seem attractive due to their easy scalability. These methods are typically classified as either covalent[25–29] or noncovalent functionalization[30–35] methods, depending on the nature of the interaction between the SWNTs and the separation agent. Noncovalent approaches are especially promising because of their ability to preserve SWNTs' inherent properties. Adsorption of molecules such as octadecylamine,[31] bromine,[32] and flavin mononucleotide[35] has achieved significant degrees of enrichment but even greater efficacy is desired. Various types of interactions such as hydrogen bonding, Van der Waals interaction, electrostatic interaction, or π-π stacking interaction between SWNTs and adsorbents are typically responsible for the selectivity. Noncovalent interactions have been observed with species selectivity with pyrene derivatives[36,37] or conjugated aromatic polymers.[38–40] However, better dispersion is required for achieving increased separation using small neutral molecules, and the relatively strong π-π interaction of the conjugated polymers is highly unfavorable with respect to postseparation removal. In addition, distinguishing the distinct contributions of different building blocks to dispersion and separation effects is impossible for conjugated polymers.

Additional Supporting Information may be found in the online version of this article.

In our previous work,[41] we suggested another kind of weak interaction associated with resonant energy transfer between polymeric chromophores and SWNTs to influence SWNT species enrichment. We have proposed that the overlap of the polymer fluorescence wavelength with the absorption wavelength of particular nanotube species results in preferential energy transfer, resulting in dipole–dipole interaction, and consequently, the polymers' selectivity toward met- or sem-SWNTs. Two polymethacrylates, specifically poly(9-anthracenylmethyl methacrylate) (PAMMA) and poly(2-naphthylmethacrylate) (PNMA), were studied (Fig. 1).[41]

In this article, two other polymethacrylates with different aromatic side groups [i.e., poly(benzyl methacrylate) (PBMA) and poly(methylmethacrylate)-*co*-(9-anthracenylmethyl acrylate) (PMMA-*c*-PAMA), Fig. 1] were investigated for their selectivity to SWNT species. The pendant groups in these polymers are UV/vis-light absorbing chromophores. The size and content of these chromophores in the four polymers are different. The SWNTs investigated were produced by the cobalt-molybdenum catalyst (CoMoCAT) method. Using PBMA and PMMA-*c*-PAMA as dispersants of SWNTs in dimethylformamide (DMF), ultraviolet/visible/near infrared (UV–vis-NIR) absorption spectra and photoluminescence excitation (PLE) maps were collected to characterize the degree of met-/sem- separation and species selectivity. The effect of solvent on semiconducting species suspension of PBMA and PMMA-*c*-PAMA was examined by PLE using two other solvents (acetonitrile and chloroform). The selectivities of the four polymethacrylates in Figure 1 were compared, and the contribution of the side group and main chain were analyzed using group contribution theory. The influence on selectivity of the standing time of the SWNTs solution after sonication was also explored.

EXPERIMENTAL

Materials

CoMoCAT SWNTs were supplied by SouthWest Nanotechnologies and were used without purification. The polymers PBMA, PNMA, PMMA-*c*-PAMA, and PAMMA as well as sodium dodecylbenzenesulfonic acid (SDBS) were purchased from Aldrich. The solvents, deuterated acetone, acetonitrile, *N*,*N*-dimethylformamide (DMF), chloroform, toluene, and deuterium oxide (D_2O), were supplied by Sino Chemical Company Pte and were used as received.

SWNTs Separation with Polymers

All separations were performed according to the following protocol: 2 mg of as-received SWNTs were mixed into 10 mL solution of polymer in DMF, followed by 10 min of sonication at 175 W and 2 weeks of standing. After the standing period, centrifugation at 20 k*g* for 1 h was performed. Both the supernatant and the precipitate fraction were collected for further characterization. The standing periods between sonication and centrifugation, which is a potential variable affecting the measured enrichment, were controlled to be 2 weeks for all selective processes.

UV–Vis-NIR absorbance spectra of suspended SWNTs were collected straightforwardly from the supernatant solution because the absorbance bands of the polymers do not overlap those of SWNTs [Fig. 2(e,f)]. SWNTs in the precipitate fraction were repeatedly washed with toluene to remove the wrapped polymer. The cleaned precipitate SWNT powders were resuspended in 1% SDBS/D_2O solution and centrifuged before UV–vis-NIR absorbance and PLE measurements.

Characterization Techniques

^1H NMR characterizations were conducted with a Bruker ACF 300FT-NMR spectrometer operating at 300 MHz. Deuterated acetone was used as the solvent with tetramethylsilane as the internal standard.

UV–Vis-NIR spectra of SWNT suspensions and polymer solutions were collected with a Cary 5000 UV–vis-NIR spectrophotometer. Polymer solution (0.1%) was used as reference for background subtraction in supernatant scans, whereas for the precipitates no background subtraction was conducted during the data collection because polymer absorption features were

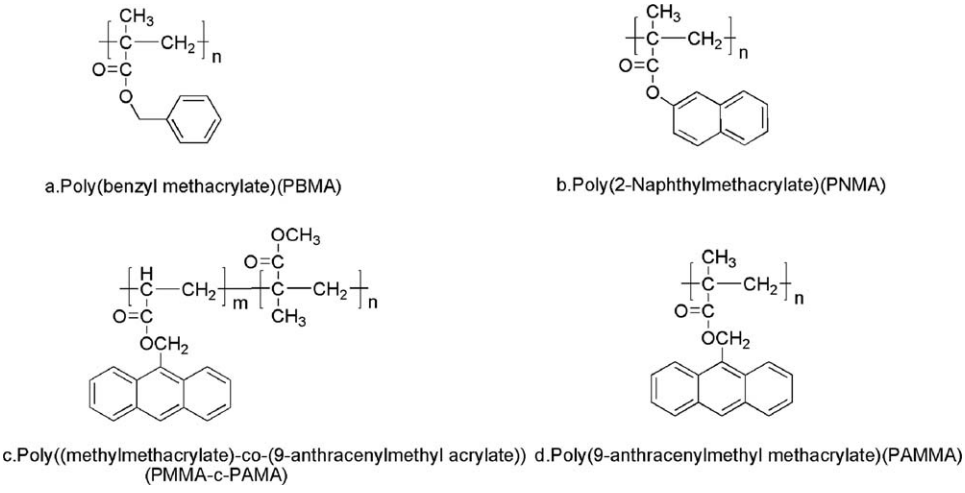

FIGURE 1 Structures of polymers used in this study.

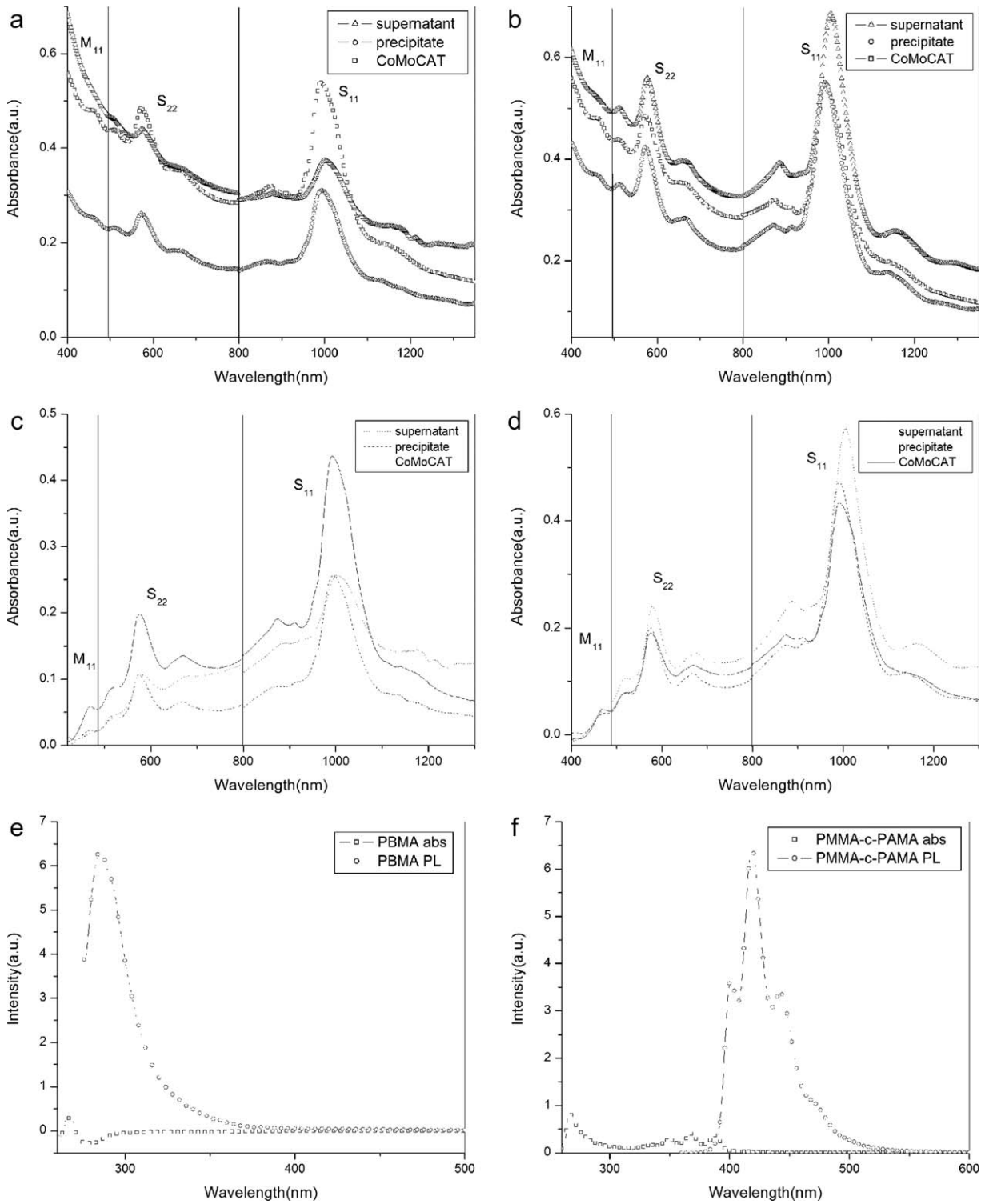

FIGURE 2 UV–vis-NIR absorbance spectra of chemically separated SWNTs. (a,b) CoMoCAT produced SWNTs in DMF with PBMA and PMMA-*c*-PAMA, respectively; (c,d) background subtracted UV–vis-NIR spectra of CoMoCAT produced SWNTs in DMF with PBMA and PMMA-*c*-PAMA, respectively; (e,f) UV–vis absorption (abs) and photoluminescence (PL) spectra of PBMA and PMMA-*c*-PAMA in DMF solution, respectively.

strongly suppressed by the toluene washing. Some of the spectra presented here have been magnified for convenient comparison; this does not affect the content ratio of different species. Because of the change of detector during data collection, a sharp edge at almost exactly 800 nm can be observed in some of the spectra.

PLE maps of the polymer suspended SWNTs and the resuspended precipitates in SDBS solution were collected with a Jobin-Yvon Nanolog-3 spectrofluorometer with an InGaAs detector.

Photoluminescence spectra of polymer solutions were obtained with an AMINCO BOWMAN II luminescence spectrometer. The samples were held in a 1 cm quartz cell during these spectral characterizations. The excitation wavelengths were 268 and 350 nm for PBMA and PMMA-*c*-PAMA, respectively.

RESULTS AND DISCUSSION

UV–Vis-NIR Spectra

UV–Vis-NIR absorption spectra of polymer suspended supernatant fraction and resuspended precipitate fraction with PBMA and PMMA-*c*-PAMA are shown in Figure 2(a,b). To more clearly see the peaks, the background is removed from the raw UV–vis-NIR data and shown in Figure 2(c,d). The UV–vis absorption and photoluminescence spectra of the neat polymers are also included [Fig. 2(e,f)] (The results for polymers PNMA and PAMMA have been previously reported by us.[41]) Also included are the absorbance spectrum of the SDBS dispersed SWNTs, which was used as reference spectrum because SDBS is believed to disperse SWNTs without any species selectivity.

The optical absorbance spectra were used for the assessment of the SWNT species abundance because the species' peak intensities above the background scale proportionally with their corresponding concentrations, regardless of whether the SWNTs are bundled or individually dispersed. The absorbance spectra exhibit absorption features due to the metallic M_{11} band as well as the semiconducting S_{11} and S_{22} bands.

All separations were carried out with the same experimental parameters such as sonication power and time, polymer solution concentration, and centrifugation conditions. Absorption spectra of the neat polymers are shown in Figure 2(e,f). PBMA and PMMA-*c*-PAMA do not affect the SWNT spectroscopic characteristics and so were not removed before spectroscopic scans of the SWNTs suspended in the supernatant solutions [Fig. 2(a–d)].

Figure 2(a,b) shows the absorbance spectra of the supernatant fraction and redispersed precipitate for PBMA and PMMA-*c*-PAMA as well as the unseparated SWNTs in SDBS solution. The CoMoCAT SWNTs exhibit prominent characteristic spectroscopic features from 400 to 510 nm for metallic SWNTs and from 510 to 1350 nm for semiconducting ones. The bands at 800–1350 nm and 510–800 nm correspond to S_{11} and S_{22}, respectively.[42–44] The ratio of the peak intensity M_{11}/S_{22} is used for the estimation of the content ratio of met- to sem-SWNTs because S_{22} is more stable spectroscopically than S_{11} to environmental doping effects. The area enclosed above the baseline in the spectra is more relevant for calculating species concentration due to the presence of the SWNT solution background, which scales approximately exponentially with the transition energy.

Our previous results[41] indicate that PNMA preferentially suspends met-SWNTs, whereas PAMMA is selective to sem-SWNTs. However, no obvious metallicity selectivity was evident from comparison of the spectra of the supernatant and resuspended precipitates resulting from treatment with separation agents PBMA and PMMA-*c*-PAMA [Fig. 2(a,b)]. The background subtracted figures [Fig. 2(c,d)] confirmed our above conclusion. Both supernatant and precipitate are slightly enriched in semiconducting SWNTs as compared with the as-received CoMoCAT SWNTs, although the degree of enrichment is a bit more obvious for supernatant suspended SWNTs. The species abundance may be resulted from some systematic error involved in sample preparation or data collection. Also, a parabolic background with "up" curvature will tend to suppress the different signature of an absorption peak, as the background has a more negative slope on the short-wavelength side of the peak than on the long-wavelength side. This could also contribute to the more obvious suppression of metallic features for supernatant suspended CoMoCAT SWNTs.

The selectivity difference among different polymers suggests that the aromatic functional groups play a critical role in the enrichment. First, the absence of metallicity selectivity with the phenyl group in PBMA, in contrast to PNMA and PAMMA,[41] indicates that the size of the chromophores is quite critical. Second, the crucial role of the content of the aromatic groups in these copolymers may be suggested by the selectivity difference between PAMMA and PMMA-*c*-PAMA. Third, the reversed metallicity selectivity for PNMA in contrast to PAMMA previously reported[41] brings out the significance of the side chromophores in the metallicity selectivity. We have postulated that selectivity is due to photon induced dipole–dipole interaction,[41] which critically depends on the overlap of the polymer fluorescence wavelength with excitation wavelength of specific SWNT species. The above observed differences can be explained by our proposed mechanism regarding the metallicity selectivity.

As compared with the as-received SWNTs, another noteworthy feature of the suspended supernatant solutions is the red shift of the SWNTs' spectroscopic peak, especially for the S_{11} peak at $\sim$1000 nm. The red shift may suggest large diameter selectivity as the SWNT bandgap scales inversely with diameter. Alternatively, it may suggest the effects of the dispersion media.[45] The PLE results, to be discussed below, show that the red shift is not a SWNT diameter selection effect so that the influence of the dispersion medium is the preferred explanation.

Photoluminescence Excitation

PLE[46–48] maps (Fig. 3) of semiconducting species in the resuspended precipitates as well as in the supernatant fraction were collected to characterize their chiral species (n,m) distributions. As-received SWNTs suspended with 1% SDBS/D_2O solution were also characterized as a reference. For the purpose of convenient comparison, species contents of various species suggested by PLE maps were estimated from their PLE signal intensities calibrated with their

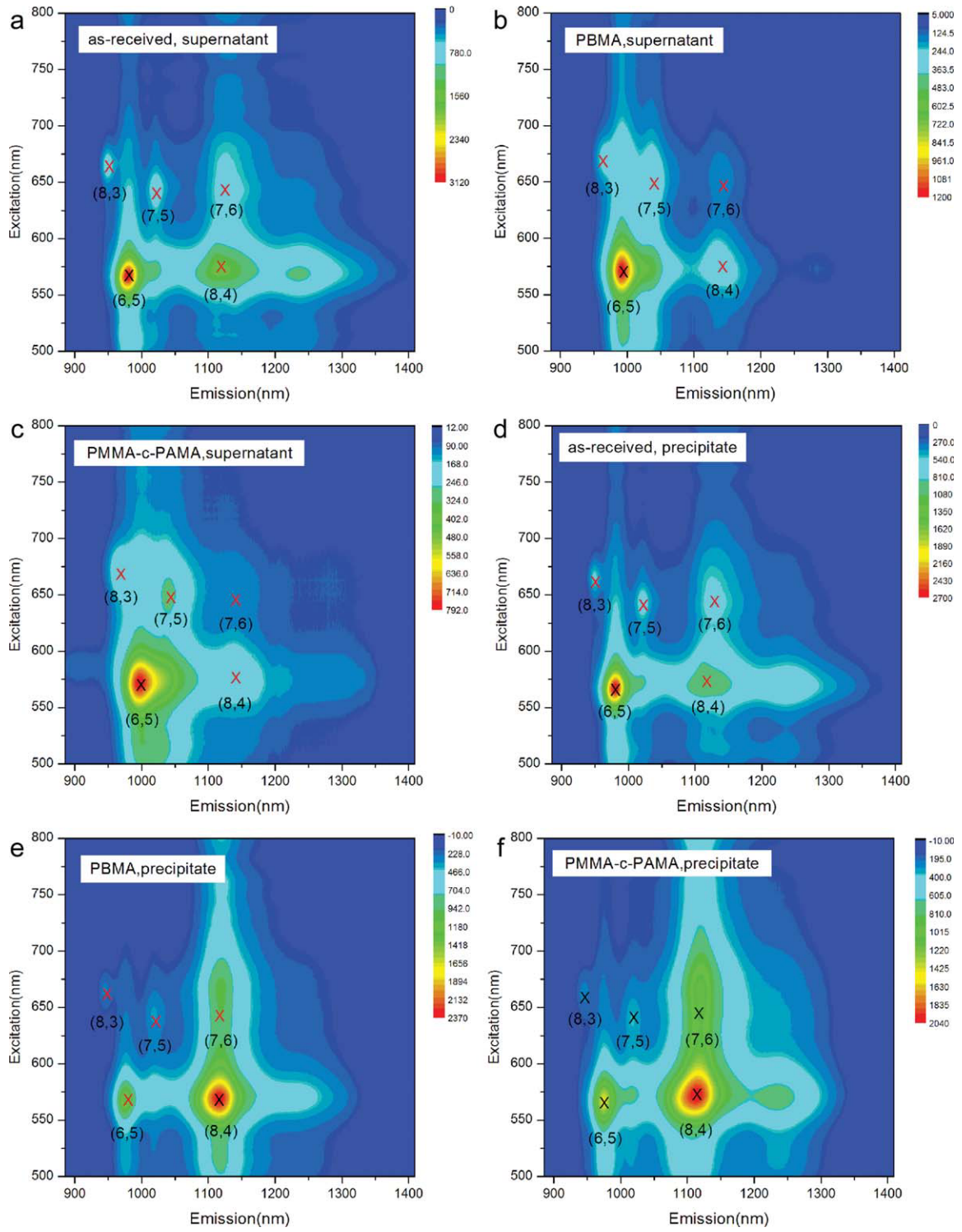

FIGURE 3 PLE maps of SWNTs dispersed with SDBS solution (a,d) and of SWNTs after chemical separation (b,c) and (e,f). (a,d) As-received CoMoCAT SWNTs dispersed using SDBS solution with supernatant fraction (a) and precipitate fraction (d). (b,c) CoMoCAT SWNTs in the supernatant solution after separation in DMF with (b) PBMA and (c) PMMA-*c*-PAMA. (e,f) CoMoCAT SWNTs precipitates after separation in DMF with (e) PBMA and (f) PMMA-*c*-PAMA.

corresponding PLE quantum efficiency, neglecting the influence of microenvironment on the PL quantum efficiency of SWNT species.[49] The calculated species abundances are tabulated in Table 1.

Typically, the as-received CoMoCAT SWNTs [Fig. 3(a,d) and Table 1] are dominated by species (6,5) and (8,4). Other species such as (8,3), (7,5), and (7,6) are also detected. Figure 3(a,d) shows quite similar species distributions and

TABLE 1 Tabulated Values of the PLE Peak Intensities and Calculated Abundances for Identified Semiconducting Species Suspended by SDBS Solution as well as Supernatant and Precipitate Fraction Separated with PBMA and PMMA-*c*-PAMA in DMF

				SDBS		PBMA				PMMA-*c*-PAMA			
						Supernatant		Precipitate		Supernatant		Precipitate	
(n,m)	d_t (nm)	θ (°)	Calculated Intensity	Experimental Intensity	Species Abundance	Experimental Intensity	Species Abundance	Experimental Intensity	Species Abundance	Experimental Intensity	Species Abundance	Experimental Intensity	Species Abundance
(6,5)	0.75	27.02	0.67	3117	42.0%	1197	51.8%	1269	19.2%	1179	47.6%	1451	22.3%
(8,4)	0.83	19.19	0.46	1550	30.4%	297	18.7%	2362	52%	491	19.8%	2037	45.6%
(8,3)	0.78	15.40	2.13	768	3.3%	272	3.7%	274	1.3%	120	4.8%	241	1.2%
(7,5)	0.82	24.54	0.71	832	10.6%	380	15.5%	369	5.3%	417	16.8%	370	5.4%
(7,6)	0.89	27.47	0.47	717	13.8%	168	10.3%	1034	22.3%	268	10.8%	1171	25.6%

indicate that SDBS suspends without species selectivity. The supernatant fraction of the SDBS suspension was selected for the reference SWNT species abundance calculation. The polymer-suspended SWNTs in the supernatant solutions [Fig. 3(b,c) and Table 1] exhibit similar modifications of the SWNT chiral species distributions: the contents of species (6,5) and (7,5) are increased by both polymers; correspondingly, the species (8,4) and (7,6), which are diminished in the supernatant, are more prominent in the PLE maps of the redispersed precipitates [Fig. 3(e–f) and Table 1]. This indicates preferential suspension of smaller diameter species by both polymers. The chiral selectivity is quite similar to our previous results with polymers PNMA and PAMMA, both of which selectively suspend species (6,5), (7,5), and (8,3).[41]

It has been reported that polymers may selectively suspend tubes with specific diameters dictated by the matching of nanotube diameter with the cavity size of polymer in its helical wrapping configuration.[50] Alternatively, the preferential wrapping of SWNTs by polymers may result from a process determined by the SWNTs' band structure as the band gap E_{11} is approximately inversely proportional to the tube diameter. Whatever the driving force, it is apparent that the polymers prefer tubes with smaller diameters. As a result, the red shift presented in the UV–vis-NIR spectra [Fig. 2(a,b) supernatant] for PBMA- and PMMA-*c*-PAMA-suspended SWNTs should be ascribed to modification of the SWNT electronic structure or other modification of the SWNT photon absorption physics when complexed with polymer.

Solvent Effect

UV–Vis-NIR absorbance spectra and the PLE maps indicate that different polymers have different species selectivities. Specifically, PAMMA preferentially disperses semiconducting SWNTs and PNMA selectively suspend metallic SWNTs,[41] whereas PBMA and PMMA-*c*-PAMA show no metallicity selectivity. Smaller diameter species are preferred by all four polymers.

Diameter selectivity of all polymers may result from the different degree of swelling of the polymer chain in different solvents of varying solvating power; the polymer size in solution is dependent on the size and structure of the aromatic side groups as well as the solvent.[51,52]

Because of the limited dispersion efficiency of these polymers, the UV–vis-NIR spectra were not well resolved and PLE maps were used to characterize the polymer suspended SWNTs in the supernatant fraction in CH_3CN and $CHCl_3$ solvents as well as in DMF (Fig. 4). Standing time was set to 2 weeks in all the tests. Also, quantitative species abundances were extracted from the PLE maps of SWNTs suspended by the polymers in $CHCl_3$ (Table 2). PLE maps of SWNTs suspended by polymers in CH_3CN were excluded from this analysis because no species other than (6,5) could be clearly identified (Fig. 4) due to the high background/signal ratio resulting from poor dispersion.

The PLE maps [Fig. 4(a–f) and Table 2] suggest that for all polymers, PBMA, PMMA-*c*-PAMA, and PAMMA, small

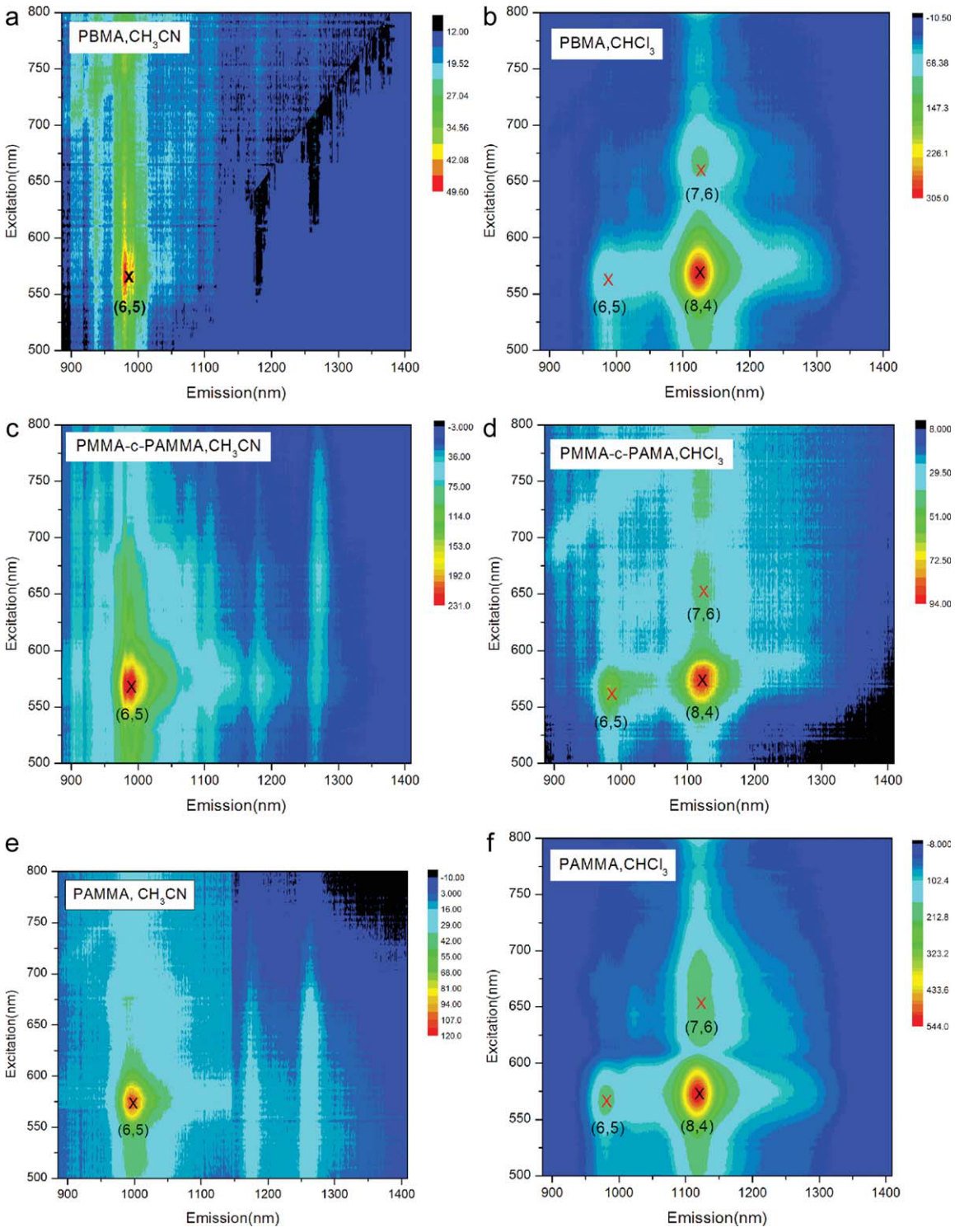

FIGURE 4 Solvent effects on the species selectivity of PBMA, PMMA-*c*-PAMA, and PAMMA. (a,b) PLE maps of the SWNTs in the supernatant fraction using PBMA with solvents (a) CH_3CN and (b) $CHCl_3$. (c,d) PLE maps of the SWNTs in the supernatant fraction using PMMA-*c*-PAMA with solvents (c) CH_3CN and (d) $CHCl_3$. (e,f) PLE maps of the SWNTs in the supernatant fraction using PAMMA with solvents (e) CH_3CN and (f) $CHCl_3$.

diameter species (6,5) is preferred in CH_3CN, whereas species with larger diameters such as (8,4) and (7,6) are selectively suspended in $CHCl_3$ (The solvent effect on PNMA has been previously investigated[41] and shows the same diameter trend.). The different selective behavior of this class of polymer, regardless of the different side functional groups, in

TABLE 2 Tabulated Values of the PLE Peak Intensities and Calculated Abundances for Identified Semiconducting Species Suspended with PBMA, PMMA-*c*-PAMA, and PAMMA in Chloroform

			PBMA		PMMA-*c*-PAMA		PAMMA	
(*n*,*m*)	d_t (nm)	θ (°)	Calculated Intensity	Experimental Intensity	Species Abundance	Experimental Intensity	Species Abundance	Experimental Intensity	Species Abundance
(6,5)	0.75	27.02	0.67	93	13.5%	64	24.4%	206	15.7%
(8,4)	0.83	19.19	0.46	304	64.2%	94	51.8%	541	60.2%
(8,3)	0.78	15.40	2.13	Not available	Not available	Not available	Not available	Not available	Not available
(7,5)	0.82	24.54	0.71	Not available	Not available	Not available	Not available	Not available	Not available
(7,6)	0.89	27.47	0.47	108	22.3%	44	23.9%	221	24.1%

different solvents is ascribed to the different degree of relaxation of the polymer chain upon dissolution in different solvents. Hansen solubility parameters (HSP) was used to investigate the solvent effects on the polymeric conformation. The prediction was made using the group contribution method.[53] Poly(methyl methacrylate) (PMMA), which is regarded as the precursor of the tested polymers, was chosen as the starting point for the calculation because its HSPs are available both experimentally and theoretically. To simplify the calculation, additive contributions of the methyl groups and various chromophore groups to the HSP of the buildup polymers, which in our case are the tested polymers and PMMA, was assumed.[53] We also neglect the difference between the HSPs of the repeating building blocks and the buildup polymers so that replacement of the methyl group contribution with that of the aromatic functional groups would permit estimation of the HSP of the tested polymers from that of PMMA. The HSP of PMMA and its component contributions as well as the estimated HSPs of our employed polymers are included (Supporting Information Tables S3, S5, and S7). The HSPs of the solvents[54] are also included (Supporting Information Tables S4, S6, and S8). The affinities between the solvents and polymers was estimated with the distance R_a[54] between the HSPs of the polymers and the solvents in Hansen space using the expression

$$R_a^2 = 4(\delta_{D_1} - \delta_{D_2})^2 + (\delta_{P_1} - \delta_{P_2})^2 + (\delta_{H_1} - \delta_{H_2})^2.$$

where δ_D, δ_P, and δ_H are the dispersion HSP, polar HSP, and the hydrogen-bonding HSP, respectively. Subscripts 1 and 2 represent the substance 1 and substance 2, that is, polymer and solvent.

The distance between the polymer and the employed solvents in Hansen space is in the increasing sequence of chloroform, DMF, and acetonitrile for all tested polymers except PMMA-*c*-PAMA. For the latter, the contribution to HSP of methyl and anthracenylmethyl groups was mole-fraction averaged over all the repeating units and we ascribed this abnormal behavior of PMMA-*c*-PAMA to the overestimation/underestimation of the averaging method of the functional groups. The polymer/solvents affinity decreases in the order $CHCl_3$, DMF, and CH_3CN. In different solvents, the diameter of the suspended species by all tested polymers decreases in the same order: larger diameter species are selectively suspended in $CHCl_3$ and smaller diameter species are preferred in CH_3CN. It is obvious that there is some straightforward relationship between polymers' species selectivity and its solvophilic property. To minimize its exposure to the solvent, the polymer shrinks in a poor solvent. This would result in the selective wrapping of the smaller diameter species (6,5) in CH_3CN as contrast to $CHCl_3$ or DMF. In the good solvent ($CHCl_3$), the tendency is reversed and larger diameter species, that is, (8,4) and (7,6) are selected. The solvent dependent characteristics of all these three polymers are consistent with our reported results with polymer PNMA.[41]

The uniform behavior of the solvent dependent diameter selectivity for all polymers suggests the dominant role of the

polymeric conformation on the diameter selectivity, although the side groups are involved in determining the affinity between polymers and solvents, as listed in the table (Supporting Information).

The different species selective behaviors of various polymers in DMF suggest that the aromatic functional groups do play some decisive role with respect to the metallicity selectivity. With naphthalene/anthracene as the side group, the polymer will selectively suspend certain SWNTs species with specific electronic properties. However, no obvious metallicity selectivity can be observed for PBMA and PMMA-*c*-PAMA, due possibly to the small aromatic functional groups (phenyl) and low loading of the anthracenyl groups in PMMA-*c*-PAMA [The anthracenylmethyl to methyl ratio of PMMA-*c*-PAMA, Fig. 1(c), was determined by its ^{1}H NMR spectra to be 3:10].

In our previous experiments, the involvement of light in the separation was identified and the role of the photon induced dipole–dipole interaction as the driven force for metallicity selectivity was suggested for this class of polymer. With this mechanism, the requirements for selectivity are twofold: first, the overlap of the polymer fluorescence with the specific nanotube species absorption,[41] and second, the energy transfer of polymer fluorescence to specific nanotube species with overlapping absorption. The diverse behavior regarding metallicity selectivity with the employed polymers can be interpreted with such criteria.

Fluorescence Spectra of Polymers

Energy transfer from the aromatic functional groups of the polymers to SWNTs can be explored with polymer fluorescence spectra. Fluorescence spectra of polymer PMMA-*c*-PAMA are shown in Figure 5(a), whereas those of polymers PNMA and PAMMA have been reported previously.[41] The polymer PBMA was excluded from this investigation because it shows no fluorescence in our interested wavelength region [Fig. 2(e)]. This means that there will be no spectral overlap between polymer fluorescence of PBMA and SWNTs absorption and no energy transfer will occur. Low concentration solutions were used in the test to reduce intermolecular interactions. The fluorescence spectra of 1.5×10^{-3} mol/L PMMA-*c*-PAMA in DMF were collected in the presence and in the absence of SWNTs (The concentration of polymer was represented by the concentration of the corresponding aromatic chromophores.). To make the fluorescence intensity comparable, all variable experimental parameters were set consistently during the spectra collection with different polymers.

From Figure 5(a), the intensity difference of the spectra represented by the triangle curve suggests strong quenching by SWNTs. For the sake of convenient comparison, the wavelength-dependent suppression factor defined as the ratio of PLE intensity in the presence of SWNTs to its intensity in the absence of SWNTs at various wavelengths for all three polymers were calculated [Fig. 5(b)]. The suppression factors of PNMA and PAMMA are significantly more variable with wavelength than is that of PMMA-*c*-PAMA.

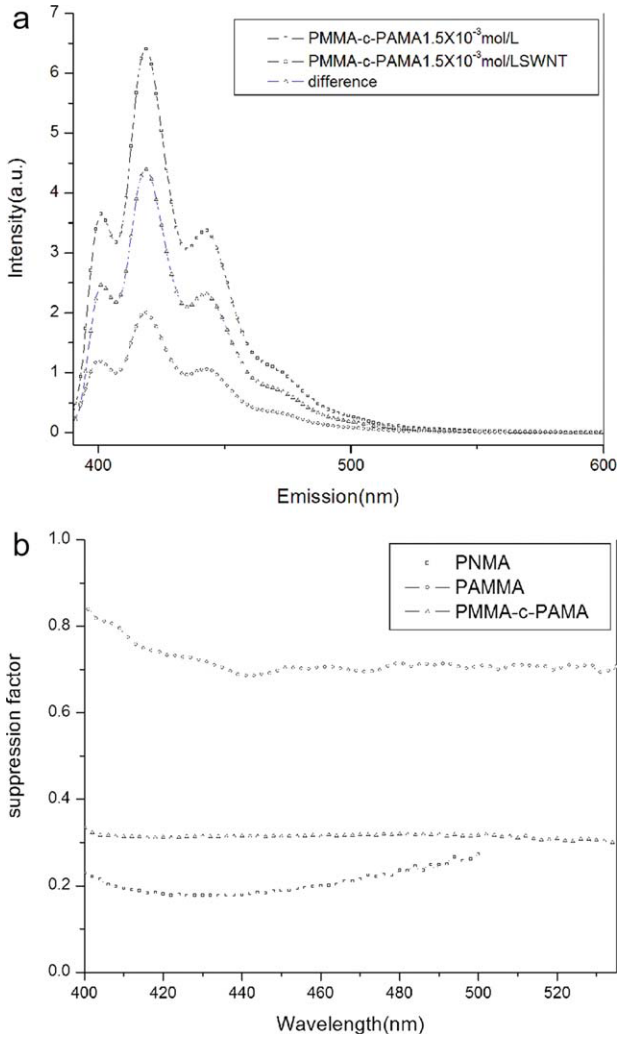

FIGURE 5 (a) Fluorescence spectra of PMMA-*c*-PAMA in the presence and in the absence of SWNTs. (b) Suppression factor of fluorescence signal intensities for all three polymers.

The nonconstant reduction in polymer fluorescence for PNMA and PAMMA in the presence of SWNTs is hypothesized to be due to energy transfer to selected SWNT species resulting from dipole–dipole interaction. The constant proportionality for PMMA-*c*-PAMA suggests that there will possibly be no selective dipole–dipole interaction between this copolymer and met- or sem-SWNTs, which is substantiated by our experimental results. Moreover, the distinction between radiative and nonradiative energy transfer suggests that nonradiative transfer,[45] which is a consequence of the dipole–dipole interaction, is more likely to be responsible for the observed metallicity selectivity for PNMA and PAMMA.[41]

Our previous results[41] indicate that for PNMA and PAMMA, the variation in fractional suppression of the polymer photoluminescence with emission wavelength indicates that it is unlikely to interpret the photoluminescence suppression by the variation in chromophore concentration or absorption/

emission cross section because the concentration of the chromophore is in its spectroscopic linear range. This corroborates our proposal of existence of some kind of coupling interaction, specifically energy transfer, between polymeric chromophore and SWNTs.

The different suppression tendency of the fluorescence for PNMA and PAMMA also suggests different interaction with SWNTs. It is the interplay of the spectral overlap and the tendency of energy transfer in energetically more favorable direction that determines the different photoluminescence suppression behaviors for PNMA and PAMMA, resulting in their distinct metallicity selectivity. Tentatively, the polymers' metallicity selectivity is ascribed to different fluorescence quenching styles, associated with which is the underlying preferential dipole–dipole interaction.

In our tested system, the induced dipole–dipole interaction may, in some situations, be present with reasonable strength in the presence of light despite the existence of van der Waals interaction and π-π stacking interaction between SWNTs and aromatic side groups. The presence of such kind of interaction ultimately results in the polymers' diverse metallicity selectivity. Moreover, the different degree of polymer conformation relaxation induced by the solvent solvation complicates the interpretation. The polymers' unique diameter and metallicity selective behavior is due to the interplay and relative scales of all involved interactions. Other factors such as electronic interaction[55,56] as well as structural compatibility may also contribute to the polymers' species discrimination. The effects of polymer backbone on the effective mapping and structural correlation between SWNTs and aromatic functional groups (involved π-π stacking interaction) may also need to be taken into consideration. For instance, the short "arm" between the polymer backbone and the anthracene groups makes its maximum contact with SWNT sidewall and optimum orientation unlikely. During the wrapping process, this type of strain effect between the polymer backbone and chromophore groups, which accompanies the attachment of functional groups onto the SWNT sidewall, may also alter their selectivity.

Standing Time Dependence

Standing time has been identified as another factor which will influence the polymers' species selectivity. UV–vis-NIR spectra and PLE maps were used to characterize different batches of separated SWNTs at different standing times after sonication. Only the polymer PNMA was selected for this investigation as its metallic species suspension decrease with standing time can be conveniently observed with UV–vis-NIR spectroscopy.

It is clear from the absorption spectra (Fig. 6) that the standing time is a critical factor for high efficiency enrichment. The degree of enrichment varied with differing standing periods of 0 day, 3 days, 1 week, and 2 weeks, with longer standing time resulting in higher selectivity by PNMA. However, PLE maps of the supernatant solution at different standing times show no change with increasing standing time (PLE maps are not shown here because they are quite similar to the map of the SWNT solution prepared with 2 weeks standing.).

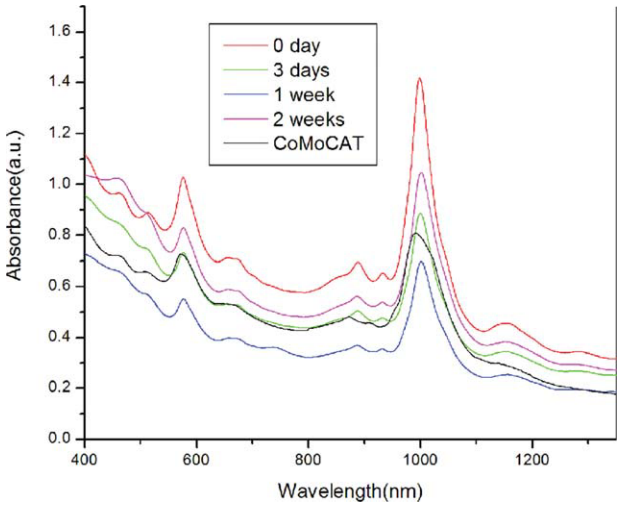

FIGURE 6 Standing time dependence characterization by UV–vis-NIR absorbance spectra of CoMoCAT produced SWNTs. Standing periods of 0 day, 3 days, 1 week, and 2 weeks for the supernatant solution with PNMA in DMF.

The tendency of metallicity selectivity improvement with increasing standing time for this polymer can be interpreted as evidence that mapping of side functional groups onto the nanotubes after sonication is necessary for the mixture to form the lowest energy wrapping states. The adjustment of the polymer backbone conformation is anticipated to be associated with the adsorption/desorption mapping throughout the process. Concisely, strong sonication results in random mapping of the aromatic functional groups onto SWNT sidewalls as well as random wrapping of segments of polymer backbones around different SWNT species, both of which suppress differential selectivity. As a result, no metallicity selectivity can be observed soon after sonication. However, due to their structural similarity, SWNTs' affinity to the aromatic side groups (π-π stacking interaction) is higher as compared with that of the polymer backbone. It can be anticipated that a lower energy conformation can be achieved by the polymer molecules adopting a "backbone outside and functional groups inside" conformation to wrap the SWNTs, provided the standing time is long enough. Diameter selectivity is the direct consequence of induced long-range wrapping of the polymer chain around SWNTs, which seems to be relatively fast from our PLE maps at different standing times. On the other hand, the presence of light will induce interaction between chromophores on the polymeric side aromatic groups and SWNTs species with specific electronic properties. Longer standing time is required for the observation of metallicity selectivity for our specific system, possibly due to the weak character of the driving force responsible for metallicity selective mapping.

The situation is further complicated by the strong π-π interaction of SWNT sidewall with the side aromatic functional groups of the polymer since this π-π interaction will result in relatively random polymer wrapping around SWNTs in the initial stages. As random wrapping is disadvantageous for the selective mapping, longer time will be required in order to achieve selectivity. It is important to point out that 2 weeks' standing time is not anticipated to be optimum and longer standing time will possibly improve the enrichment efficiency. However, 2 weeks' standing enables us to observe the SWNT species enrichment in an acceptable period (relatively short) and was thus used in this report.

CONCLUSIONS

Four polymethacrylates with different aromatic side groups (PBMA, PNMA, PMMA-*c*-PAMA, and PAMMA) have been used here and, in our previous study,[41] in the electronic properties (met-/sem-) and diameter based species selection of SWNTs. Effective enrichment has been achieved. UV–vis-NIR absorbance spectra and PLE maps suggest that these polymers have strong preferentiality to certain SWNTs species and the species selectivity depends on the polymer/solvent combination. In DMF, we previously showed that PAMMA preferentially disperses semiconducting SWNTs and PNMA selectively suspends metallic SWNTs, whereas PBMA and PMMA-*c*-PAMA are shown in this paper to have no metallicity selectivity. All four polymers selectively suspend species with smaller diameters. Their selective behavior is quite sensitive to the solvent employed and highly similar tendency in diameter preference is observed upon change of solvents. For all four polymers in CH_3CN, PLE spectra show that the semiconducting species suspended are mainly of smaller diameters, whereas in $CHCl_3$, extracted semiconducting species are mainly of larger diameters. The parallel relationship between the diameters of the extracted species and the affinity between the polymers and solvents substantiate our argument that the uniform behavior of the solvent dependent diameter selectivity results from the conformation relaxation of polymer chain in solvents, which is believed to be mainly determined by the polymer backbone although the side groups do make some non-negligible contribution. On the contrary, the different species selective behaviors of various polymers in DMF suggest that the aromatic functional groups play some decisive role with respect to the metallicity selectivity. Both aromatic ring size and loading of the chromophores are essential factors. We propose that photon induced coupling is potentially responsible for their discrimination between met- and sem-SWNTs. Other factors, that is, structural compatibility (simultaneous optimization of the effective mapping and structural correlation between SWNTs and aromatic functional groups) or electronic interaction,[55,56] and so forth cannot be totally excluded from the contribution to polymers' species selective behavior and further study is required. Nevertheless, these polymethacrylates with pendant aromatic side groups facilitate the dissection of the contribution to chiral selectivity from the side chain and main chain constituents. Systematic study of the various chemical units' contribution to the separation effect is thus possible with rationally designed polymer structure. Standing time of the SWNTs solution after sonication is identified as another critical factor for the species enrichment.

ACKNOWLEDGMENTS

The work was supported by a Competitive Research Program grant from the Singapore National Research Foundation (NRF-CRP2-2007-02). X. Pan acknowledges the support of Nanyang Technological University through a Research Scholarship.

REFERENCES AND NOTES

1 White, C. T.; Todorov, T. N. *Nature* **1998,** *393*, 240–242.

2 Quinn, B. M.; Lemay, S. G. *Adv. Mater.* **2006,** *18*, 855–859.

3 Pop, E.; Mann, D.; Wang, Q.; Goodson, K.; Dai, H. J. *Nano Lett.* **2006,** *6*, 96–100.

4 Yu, M. F.; Lourie, O.; Dyer, M. J.; Moloni, K.; Kelly, T. F.; Ruoff, R. S. *Science* **2000,** *287*, 637–640.

5 Pan, Z. W.; Xie, S. S.; Lu, L.; Chang, B. H.; Sun, L. F.; Zhou, W. Y.; Wang, G.; Zhang, D. L. *Appl. Phys. Lett.* **1999,** *74*, 3152–3154.

6 Poncharal, P.; Wang, Z. L.; Ugarte, D.; de Heer, W. A. *Science* **1999,** *283*, 1513–1516.

7 Walters, D. A.; Ericson, L. M.; Casavant, M. J.; Liu, J.; Colbert, D. T.; Smith, K. A.; Smalley, R. E. *Appl. Phys. Lett.* **1999,** *74*, 3803–3805.

8 Artukovic, E.; Kaempgen, M.; Hecht, D. S.; Roth, S.; Gruner, G. *Nano Lett.* **2005,** *5*, 757–760.

9 Takenobu, T.; Takahashi, T.; Kanbara, T.; Tsukagoshi, K.; Aoyagi, Y.; Iwasa, Y. *Appl. Phys. Lett.* **2006,** *88*, 033511-513.

10 Iijima, S. *Nature* **1991,** *354*, 56–58.

11 Durkop, T.; Getty, S. A.; Cobas, E.; Fuhrer, M. S. *Nano Lett.* **2004,** *4*, 35–39.

12 Bradley, K.; Gabriel, J. C. P.; Gruner, G. *Nano Lett.* **2003,** *3*, 1353–1355.

13 Cao, Q.; Kim, H. S.; Pimparkar, N.; Kulkarni, J. P.; Wang, C. J.; Shim, M.; Roy, K.; Alam, M. A.; Rogers, J. A. *Nature* **2008,** *454*, 495.

14 Zhou, Y. X.; Gaur, A.; Hur, S. H.; Kocabas, C.; Meitl, M. A.; Shim, M.; Rogers, J. A. *Nano Lett.* **2004,** *4*, 2031–2035.

15 Cao, Q.; Rogers, J. A. *Adv. Mater.* **2009,** *21*, 29–53.

16 Avouris, P. *Acc. Chem. Res.* **2002,** *35*, 1026–1034.

17 Saito, R.; Fujita, M.; Dresselhaus, G.; Dresselhaus, M. S. *Appl. Phys. Lett.* **1992,** *60*, 2204–2206.

18 Li, Y. M.; Mann, D.; Rolandi, M.; Kim, W.; Ural, A.; Hung, S.; Javey, A.; Cao, J.; Wang, D. W.; Yenilmez, E.; Wang, Q.; Gibbons, J. F.; Nishi, Y.; Dai, H. J. *Nano Lett.* **2004,** *4*, 317–321.

19 Krupke, R.; Hennrich, F.; von Lohneysen, H.; Kappes, M. M. *Science* **2003,** *301*, 344–347.

20 Lee, D. S.; Kim, D. W.; Kim, H. S.; Lee, S. W.; Jhang, S. H.; Park, Y. W.; Campbell, E. E. B. *Appl. Phys. A* **2005,** *80*, 5–8.

21 Lutz, T.; Donovan, K. J. *Carbon* **2005,** *43*, 2508–2513.

22 Zheng, M.; Jagota, A.; Strano, M. S.; Santos, A. P.; Barone, P.; Chou, S. G.; Diner, B. A.; Dresselhaus, M. S.; McLean, R. S.; Onoa, G. B.; Samsonidze, G. G.; Semke, E. D.; Usrey, M.; Walls, D. J. *Science* **2003,** *302*, 1545–1548.

23 Zheng, M.; Semke, E. D. *J. Am. Chem. Soc.* **2007,** *129*, 6084–6085.

24 Arnold, M. S.; Green, A. A.; Hulvat, J. F.; Stupp, S. I.; Hersam, M. C. *Nat. Nanotechnol.* **2006,** *1*, 60–65.

25 Strano, M. S.; Dyke, C. A.; Usrey, M. L.; Barone, P. W.; Allen, M. J.; Shan, H. W.; Kittrell, C.; Hauge, R. H.; Tour, J. M.; Smalley, R. E. *Science* **2003,** *301*, 1519–1522.

26 Menard-Moyon, C.; Izard, N.; Doris, E.; Mioskowski, C. J. *Am. Chem. Soc.* **2006,** *128*, 6552–6553.

27 An, L.; Fu, Q. A.; Lu, C. G.; Liu, J. J. *Am. Chem. Soc.* **2004,** *126*, 10520–10521.

28 Kim, W. J.; Usrey, M. L.; Strano, M. S. *Chem. Mater.* **2007,** *19*, 1571–1576.

29 Hemraj-Benny, T.; Wong, S. S. *Chem. Mater.* **2006,** *18*, 4827–4839.

30 Maeda, Y.; Kimura, S.; Kanda, M.; Hirashima, Y.; Hasegawa, T.; Wakahara, T.; Lian, Y. F.; Nakahodo, T.; Tsuchiya, T.; Akasaka, T.; Lu, J.; Zhang, X. W.; Gao, Z. X.; Yu, Y. P.; Nagase, S.; Kazaoui, S.; Minami, N.; Shimizu, T.; Tokumoto, H.; Saito, R. J. *Am. Chem. Soc.* **2005,** *127*, 10287–10290.

31 Chattopadhyay, D.; Galeska, L.; Papadimitrakopoulos, F. J. *Am. Chem. Soc.* **2003,** *125*, 3370–3375.

32 Chen, Z. H.; Du, X.; Du, M. H.; Rancken, C. D.; Cheng, H. P.; Rinzler, A. G. *Nano Lett.* **2003,** *3*, 1245–1249.

33 Li, H. P.; Zhou, B.; Lin, Y.; Gu, L. R.; Wang, W.; Fernando, K. A. S.; Kumar, S.; Allard, L. F.; Sun, Y. P. *J. Am. Chem. Soc.* **2004,** *126*, 1014–1015.

34 Zhang, Z. B.; Zhang, S. L. *J. Am. Chem. Soc.* **2007,** *129*, 666–671.

35 Ju, S. Y.; Doll, J.; Sharma, I.; Papadimitrakopoulos, F. *Nat. Nanotechnol.* **2008,** *3*, 356–362.

36 Chen, R. J.; Zhang, Y. G.; Wang, D. W.; Dai, H. J. *J. Am. Chem. Soc.* **2001,** *123*, 3838–3839.

37 Wang, W.; Fernando, K. A. S.; Lin, Y.; Meziani, M. J.; Veca, L. M.; Cao, L.; Zhang, P.; Kimani, M. M.; Sun, Y. P. *J. Am. Chem. Soc.* **2008,** *130*, 1415–1419.

38 Nish, A.; Hwang, J. Y.; Doig, J.; Nicholas, R. J. *Nat. Nanotechnol.* **2007,** *2*, 640–646.

39 Hwang, J. Y.; Nish, A.; Doig, J.; Douven, S.; Chen, C. W.; Chen, L. C.; Nicholas, R. J. *J. Am. Chem. Soc.* **2008,** *130*, 3543–3553.

40 Chen, F. M.; Wang, B.; Chen, Y.; Li, L. J. *Nano Lett.* **2007,** *7*, 3013–3017.

41 Pan, X.; Li, L.-J.; Chan-Park, M. B. *Small* **2010,** *6*, 1311–1320.

42 Hennrich, F.; Krupke, R.; Lebedkin, S.; Arnold, K.; Fischer, R.; Resasco, D. E.; Kappes, M. *J. Phys. Chem. B* **2005,** *109*, 10567–10573.

43 O'Connell, M. J.; Bachilo, S. M.; Huffman, C. B.; Moore, V. C.; Strano, M. S.; Haroz, E. H.; Rialon, K. L.; Boul, P. J.; Noon, W. H.; Kittrell, C.; Ma, J. P.; Hauge, R. H.; Weisman, R. B.; Smalley, R. E. *Science* **2002,** *297*, 593–596.

44 Bachilo, S. M.; Strano, M. S.; Kittrell, C.; Hauge, R. H.; Smalley, R. E.; Weisman, R. B. *Science* **2002,** *298*, 2361–2366.

45 Valeur, B. Molecular Fluorescence: Principles and Applications; Wiley-VCH Verlag GmbH: Weinheim, Germany, **2001.**

46 Weisman, R. B.; Bachilo, S. M. *Nano Lett.* **2003,** *3*, 1235–1238.

47 Jones, M.; Engtrakul, C.; Metzger, W. K.; Ellingson, R. J.; Nozik, A. J.; Heben, M. J.; Rumbles, G. *Phys. Rev. B* **2005,** *71*.

48 Miyauchi, Y.; Oba, M.; Maruyama, S. *Phys. Rev. B* **2006,** *74*.

49 Oyama, Y.; Saito, R.; Sato, K.; Jiang, J.; Samsonidze, G. G.; Gruneis, A.; Miyauchi, Y.; Maruyama, S.; Jorio, A.; Dresselhaus, G.; Dresselhaus, M. S. *Carbon* **2006,** *44*, 873–879.

50 Yan, L. Y.; Li, W. F.; Fan, X. F.; Wei, L.; Chen, Y.; Kuo, J. L.; Li, L. J.; Kwak, S. K.; Mu, Y. G.; Chan-Park, M. B. *Small* **2010,** *6*, 110–118.

51 Traiphol, R.; Sanguansat, P.; Srikhirin, T.; Kerdcharoen, T.; Osotchan, T. *Macromolecules* **2006,** *39*, 1165–1172.

52 Quan, S. Y.; Teng, F.; Xu, Z.; Qian, L.; Hou, Y. B.; Wang, Y. S.; Xu, X. R. *Eur. Polym. J.* **2006,** *42*, 228–233.

53 Stefanis, E.; Panayiotou, C. *Int. J. Thermophys.* **2008,** *29*, 568–585.

54 Hansen, C. M. Hansen Solubility Parameters: A User's Handbook; CRC Press: Boca Raton, Florida, **2000.**

55 Lu, J.; Nagase, S.; Zhang, X. W.; Wang, D.; Ni, M.; Maeda, Y.; Wakahara, T.; Nakahodo, T.; Tsuchiya, T.; Akasaka, T.; Gao, Z. X.; Yu, D. P.; Ye, H. Q.; Mei, W. N.; Zhou, Y. S. *J. Am. Chem. Soc.* **2006,** *128*, 5114–5118.

56 Lu, J.; Lai, L.; Luo, G.; Zhou, J.; Qin, R.; Wang, D.; Wang, L.; Mei, W. N.; Li, G.; Gao, Z.; Nagase, S.; Maeda, Y.; Akasaka, T.; Yu, D. *Small* **2007,** *3*, 1566–1576.